A free-surface solar pond model with a sloping edge: model code and data

Koen Hilgersom, Francisco Suárez, Marcel Zijlema,
Mark Hausner, Scott Tyler and Nick van de Giesen

June 21, 2017

Abstract

A non-hydrostatic free-surface model was set up to simulate salt and heat transport in a solar pond in order to: 1) investigate the added value of free-surface models for these types of simulations, and 2) assess the importance of heat transport along a sloping side wall. This data set presents the source code, the raw measurement and model data, and several movies comparing the vertical two-dimensional (2DV) model simulations to the measurements. To demonstrate the added value of a free surface approach, this data set includes model results for both free surface and rigid-lid simulations. The presented model code is an extension of the SWASH non-hydrostatic model, which is briefly introduced in this document. A complete discussion of the model results and conclusions are provided in an accompanying article.

1 Introduction

Salt-gradient solar ponds store thermal energy from shortwave solar radiation, which penetrates the water body, in their hypersaline bottom layer (Suárez et al., 2010). The top fresh layer in the stratified water body functions as an insulator. This way, a solar pond is an efficient means to store thermal energy, which can be regained from the pond with a heat exchanger.

Solar ponds can function because of double-diffusive convection. This physical phenomenon occurs when a denser saline and warm layer is located underneath a fresher and colder layer. Where diffusion would normally erode the interface between the layers over time, the onset of convection in the layers maintains a sharp interface. In other words, the convective flows in a solar pond suppress mixing processes.

In the case of a sloping side wall, heat transport along the slope could counteract the optimal functioning of the pond. When a solar pond is large enough, the effect is assumed negligible. However, only few modeling studies have been performed in the past to assess the effect of a sloping side wall. The presented

data set combines model simulations and measurements to investigate how the slope leads to additional heat loss from the lower convective zone.

A non-hydrostatic modeling approach aids in accurately resolving flows in water bodies with large density gradients, and is expected to improve the flow simulations. The SWASH non-hydrostatic model code is open source, which allows to extend the code for the current application. SWASH solves the Navier-Stokes equations with a free surface and was originally developed to simulate the wave run-up on shores, which is beneficial for the flow simulations along the sloping edge and in particular at its intersection with the water surface. The mass and momentum conservative modeling framework is required to accurately simulate the transport of heat and salt in the pond. The modeling study therefore also serves to investigate the merit of free-surface modeling for the processes occurring in a pond with large density gradients.

The SWASH source code was extended to allow the simulation of heat exchange with the environment and more accurately calculate the density, viscosity, diffusivity, and heat capacity throughout the model domain, which are dependent on the temperature and salinity. Moreover, the model code now provides a setting to enforce a rigid-lid simulation. The extended source code and the results of the case studies are part of this data set. This document briefly describes the extension of the SWASH code and the additional commands available to run the model. The results are discussed in an accompanying article.

2 Model description and use

2.1 SWASH

The open source non-hydrostatic model SWASH is developed to simulate near-shore wave fields and rapidly varied flows (SWASH source code (Version 1.20), 2011; Zijlema et al., 2011). The SWASH model was selected for these simulations for the following reasons:

1. the code is open source and can be extended for free under the GNU GPL license;
2. SWASH offers the opportunity to solve the Navier-Stokes equation in a 2DV grid set-up;
3. the solution procedure is momentum and mass conservative, which is a requirement for proper transport modeling;
4. flows in water bodies with large density gradients are resolved accurately because of the non-hydrostatic solution procedure.

Several publications describe the governing equations, the computational approach and the potential fields of application of SWASH (e.g., Stelling and Zijlema, 2010; Zijlema et al., 2011).

2.2 Model code

2.2.1 General code extensions

The SWASH source code is downloadable from `http://swash.sourceforge.net/`. The extended source code is available in this data set in the folder 'Model source code and executables/source code'. A compiled version of the code that can be run directly as an executable is available in the folder 'Model source code and executables/executables', both for serial and parallel computing.

Most notably, the modified transport and density modules allow an accurate smaller-scale transport modeling. Please note that the modifications are made to an earlier version of SWASH, and future updates of the official SWASH code are foreseen, which will not be applied to the source code available in this data set.

The transport modules are completely renewed and include temperature increments via source terms. These source terms are calculated in an additional module (SwashRadiance2.ftn90) based on radiation data and including heat exchange with the environment at the boundaries based on temperature data (Subsection 2.2.2). Diffusion is now calculated based on the sum of molecular and turbulent diffusivities, although the current application did not apply a turbulence model. The molecular diffusivities are calculated based on their physical relation with salinity and temperature, and they are updated each time step from the salinity and temperature states in 'SwashUpdateDiffCoAndHeatCap.ftn90'. Optionally, the turbulent diffusivities are calculated by dividing the eddy viscosity by the Prandtl-Schmidt number.

The density module originally applies the Eckart formula to calculate the density states from temperature and salinity (Eckart, 1958). In the current version, the updated Eckart formula is implemented (Wright, 1997), which is based on the UNESCO formula for density (Unesco, 1981).

A coefficient alfa was added to the module that solves the momentum equations, which allows to vary the surface condition from completely rigid-lid (alfa = 0) towards a free variation (free surface: alfa = 1). Currently, the value of alfa can only be set within the model script itself. Therefore, one needs to be able to compile the model script when one wants to set the value of alfa (standard setting: alfa = 1).

2.2.2 Solar radiation and heat exchange module

The new module SwashRadiance2.ftn90 calculates the temperature increments from solar radiation, heat exchange with the atmosphere, and heat exchange through the pond bed and walls. The following lists the included heat fluxes:

- The extinction of short-wave radiation Q_{SWR} (W m^{-2}) over depth z (m) is calculated according to the equation presented by Rabl and Nielsen (1975):

$$Q_{SWR}(z) = Q_{SWR;0} \cdot \sum_{i=1}^{3} (1 - A_{SWR;i}) \cdot \frac{\eta_i}{100} \cdot \exp(-\mu_i \cdot z)$$

Table 1: Extinction coefficients μ (m^{-1}) and reflectivities A_{SWR} (-) for the artificial SWR divided over three ranges of wavelengths λ (nm), each representing η % of the total SWR penetrating the surface water body.

λ(nm)	A_{SWR} (-)	η (%)	μ (m^{-1})
350 - 440	0.015	5.54	6.43
440 - 685	0.121	71.75	1.89
$>$ 685	0.021	22.71	7.21

However, the current implementation applies different extinction coefficients μ (m^{-1}), wavelength spectrum fractions η (%), and reflectivities A_{SWR} (-) to account for the extinction of shortwave radiation (Table 1). The coefficients that are applicable for solar radiation still need to be implemented for simulating outdoor environments. In the current case, the measured incoming short-wave radiation $Q_{SWR;0}$ was reduced by 20% to account for radiation losses over the depth between the sensor and the water surface.

- The heat increment due to longwave radiation exchange with the atmosphere Q_{LWR} (W m^{-2}) is calculated according to Henderson-Sellers (1986):

$$Q_{LWR} = \sigma \cdot \left((1 - A_{LWR}) \cdot \varepsilon_a \cdot T_a^4 - \varepsilon_w \cdot T_w^4 \right)$$

with the reflectivity $A_{LWR} = 0.03$ (-) for incoming longwave radiation, atmospheric emissivity ε_a (-), water surface emissivity $\varepsilon_w = 0.972$ (-), Stefan-Boltzmann constant $\sigma = 5.6697 \cdot 10^{-8}$ W m^{-2} K^{-4}, air temperature above the pond T_a (K) and water surface temperature T_w (K). In the current application, the 'atmospheric emissivity' is set to $\varepsilon_a = 0.85$ for the emissivity of the concrete ceiling. The code includes lines to calculate the atmospheric emissivity according to Henderson-Sellers (1986), which should be uncommented for outdoor applications.

- The latent or evaporative heat flux Q_{evap} (W m^{-2}) is calculated according to Adams et al. (1990). For outdoor applications, wind-induced evaporation should still be implemented. For the current indoor application, wind-forced convection is assumed negligible. Hence, the latent heat flux is equal to the heat flux induced by free convection:

$$Q_{evap} = \begin{cases} -2.7 \cdot 10^{-2} \cdot (T_{wv} - T_{av})^{1/3} \cdot (e_{sw} - e_a) & T_{wv} > T_{av} \\ 0 & T_{wv} \leq T_{av} \end{cases} \quad (1)$$

with virtual water and air temperatures T_{wv} and T_{av} (K), respectively, and with air vapor pressure e_a (Pa) and saturated vapor pressure at the water surface e_{sw} (Pa) calculated according to Henderson-Sellers (1986): $e_a = \psi \cdot 2.1718 \cdot 10^{10} \cdot \exp\left(\frac{-4157}{T_a - 33.91}\right)$

$e_{sw} = 2.1718 \cdot 10^{10} \cdot \exp\left(\frac{-4157}{T_w - 33.91}\right)$
with the relative humidity ψ (-). The code that is published in the data set only accounts for evaporation rate in terms of heat loss and does not account for the change in water volume.

- The conductive heat flux across the water surface Q_{cond} (W m^{-2}) is calculated according to Thomann and Mueller (1987). For outdoor applications, wind-induced heat conduction should still be implemented (Kim and Chapra, 1997). For the current indoor application, wind-forced heat conduction is assumed negligible. Therefore, only the free convective part is modeled:

$$Q_{cond} = -c_1 \cdot 19.0 \cdot (T_w - T_a) \tag{2}$$

with Bowen's coefficient $c_1 = 62$ Pa K^{-1}.

- Besides conductive heat transfer over the water surface, the heat conduction through the pond's side walls and bottom Q_{wall} (W m^{-2}) is included in the calculations:

$$Q_{wall} = \frac{T_w - T_{lab}}{c_r} \tag{3}$$

where T_{lab} (K) is the solar pond's ambient temperature and $c_r = 3.36$ K m^2 W^{-1} is the conductive heat resistance factor for the insulating pond wall material.

The sum of the net heat fluxes is converted to source terms in the heat transport module by means of its physical relationship for each time step $\triangle t$ (s):

$$\frac{\triangle T}{\triangle t} = \frac{Q_{LWR;i} + Q_{LWR;e} + Q_{evap} + Q_{cond} + Q_{SWR} + Q_{wall;ver}}{c \cdot \rho \cdot \triangle z} + \frac{Q_{wall;hor}}{c \cdot \rho \cdot \triangle x} \tag{4}$$

where a distinction is made between the vertical (ver) and horizontal (hor) wall conduction, as they should be divided over the cell depths ($\triangle z$) and cell widths ($\triangle x$), respectively. The salinity- and temperature-dependent specific heat capacity c (J kg^{-1} K^{-1}) is calculated from the temperature and salinity states in 'SwashUpdateDiffCoAndHeatCap.ftn90'. The applied equation follows from a linear regression to data presented in the International Critical Tables of Numerical Data, Physics, Chemistry and Technology (Washburn and West, 1933):

$$c = 4184.92 + 2.05411 \cdot 10^{-1} \cdot T - 3.16068 \cdot 10^{-4} \cdot T^2 - 57.5177 \cdot S + 9.93871 \cdot 10^{-1} \cdot S^2 \tag{5}$$

2.3 Running the model

This data set offers the extended model as executables for single and multi core computing. Alternatively, one can optionally modify and compile the FORTRAN source code in this data set. For compiling, we refer to the SWASH implementation manual. Version 3.14 of the implementation manual is part of the documentation in this data set. The most recent version of the implementation manual is available from the SWASH online documentation (`http://swash.sourceforge.net/online_doc/swashimp/swashimp.html`).

SWASH is executed from a command file. The SWASH user manual describes how to set up such a command file. The command file used for the presented solar pond simulations and Version 3.14AB of the user manual are available from this data set. The most recent version of the user manual is available from the SWASH online documentation (`http://swash.sourceforge.net/online_doc/swashuse/swashuse.html`).

Compared to the user manual, the extended code provides several additional options for the INPgrid and READinp commands in the command file:

INPgrid	(<	RADiation RHCC (Relative Humidity and Cloud Cover) TEMPerature	>)
READinp	(<	RADiation RHCC (Relative Humidity and Cloud Cover) TEMPerature	>)

With these command options, the user provides SWASH with additional atmospheric boundary data:

RADiation — this option defines the input grid for the shortwave radiation data (INPgrid), and allows the user to indicate that the shortwave radiation data are to be read from the file (READinp; the sign of the input can be changed with option [fac] = −1).

RHCC — this option defines the input grid for the relative humidity and cloud cover data (INPgrid), and allows the user to indicate that the relative humidity and cloud cover data are to be read from the file (READinp; the sign of the input can be changed with option [fac] = −1). Here, the relative humidity and cloud cover, respectively, are imported in the same manner as any variable with two dimensions (e.g., the velocity in two horizontal dimensions defined by CURrent).

TEMPerature — this option defines the input grid for the air temperature and water temperature data (INPgrid), and allows the user to indicate that the air and water temperature data are to be read from the file (READinp; the sign of the input can be changed with option [fac] = −1). Here, the air and water temperatures, respectively, are imported in the same manner as any variable with two dimensions (e.g., the velocity in two horizontal dimensions defined by CURrent).

Table 2: Raw model output data files. Lines in *italics* indicate additional files, which serve as supporting information (i.e., they are not direct model output).

File name	Variable	Unit	Number of values		Vertical location
			x-dir.	z-dir.	
swashSolTDEP.tbl	Time	yyyymmdd. HHMMSS[a]	203	1	-
	Water level	m	203	1	water surface
swashSolVEL.tbl	Velocity (x-direction)	$m\,s^{-1}$	203	86	cell center
	Velocity (y-direction)	$m\,s^{-1}$	203	86	cell center
	Velocity (z-direction)	$m\,s^{-1}$	203	87	cell interface
swashSolTEMP.tbl	Temperature	^oC	203	86	cell center
swashSolSALT.tbl	Salinity	weight-‰	203	86	cell center
swashSolINTDEP.tbl	*Interface depths (t=0)*	m	*203*	*87*	*cell interface*

[a] y = year; m = month; d = day; H = hour; M = minute; S = second.

3 Data

3.1 Model data

The raw model output for the free surface and rigid-lid simulations is presented in text files (*.tbl) in the folder 'Model data'. Table 2 gives an overview of the data and indicates whether the data in vertical (z) direction are defined on the cell interfaces or in the cell centers. Because most cell depths are defined relative to the water depth, the vertical cell locations vary over time, and the absolute grid locations of the data can not be presented in this data set. 'swashSolINTDEP.tbl' (last row in Table 2) gives an example of the grid interface locations for the initial water depths. The complete (mixed relative and absolute) grid definition can be found in the command file 'swashSolarPond.sws' in the folder 'Model source code and executables/command file', which is the SWASH command file that was called for the free surface and the rigid-lid simulations. This file also contains all the other settings that were applied for the model simulation.

The data set further includes a Matlab routine that plots the data as *.avi movie files ('mkplotV7.m') or *.eps figure files ('mkplot_EPS.m') in the folder 'Matlab routine for plotting the Swash output'. A special routine sets up a movie or a series of EPS figures compares the model data to the measurement data ('mkplotComp_V1.m' and 'mkplotComp_EPS.m'). These files are used to create the movies of the model results in the data set and the graphical output in Section 4.

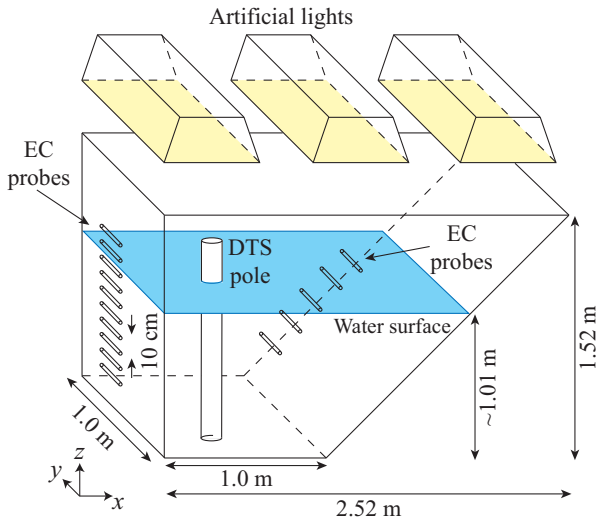

Figure 1: The laboratory set-up with the locations of the sensors.

3.2 Measurement data

Laboratory experiments to the functioning of a side-sloped solar pond were performed in March 2009. The insulated laboratory-scale solar pond had one sloping side wall (45°) on the right, a vertical side wall on the left, and two vertical parallel side walls in the front and in the back (Figure 1). The pond was heated from above by three high-intensity discharge lamps (Super Grow 1000 W, Hydrofarm Inc., Petaluma, CA). Air temperature and relative humidity were measured using a shielded sensor (HPMC45-L, Campbell Sci., Logan, UT). The net shortwave radiation and longwave radiation were measured with two pyranometers (LP02, Hukseflux, Delft, the Netherlands) and one net radiometer (Q-7.1, Campbell Sci., Logan, UT) at 0.2 m above the water surface. In this data set, the measured short-wave radiation, relative humidity, as well as measured temperatures above and just below the water surface are already converted to text files (*.tbl), which serve directly as an input for the model simulations. These files can be found in the folder 'Model source code and executables/command file'.

During the laboratory experiments, temperature and electrical conductivity (EC) data were taken at different depths above the flat bottom and along the sloping wall of the pond with fifteen EC electrodes (SK23T, Van London-Phoenix Company, Houston, TX), which were installed in one of the parallel side walls of the pond (Figure 1). The EC values were corrected to a reference temperature of 25 ^oC. Because of the high EC values, no equation was found to convert these values to salinities. Therefore, the EC data was converted to salinity (S) data with a rough linear conversion constant $K = S/EC = 0.6$, in order to compare the data with the modeled salinities.

Apart from the point measurements performed with the EC electrodes, temperature data was measured with a coiled fiber-optic cable according to the principle of distributed temperature sensing (DTS). This 'DTS pole' was located above the flat bottom at $x \approx 36\,cm$ from the left vertical side wall and $y \approx 23\,cm$ from the front parallel side wall (Figure 1). Additionally, water samples were taken several times during the experiments to analyze the water density at several depths with a portable density meter (DA-110M, Mettler Toledo, Columbus, OH). The measured density profile can be compared to the water density values calculated by the model.

The EC electrode data, DTS pole data, and density data are made available as NetCDF files (*.nc) in the folder 'Measurement data'. Besides they are converted to a Matlab data file that allows comparison with the model output in the folder 'Matlab routine for plotting the Swash output/Comparing Swash output'. The NetCDF file for the DTS measurements contains data on the raw Stokes, anti-Stokes, and temperature data against the time and the distance along the fiber-optic cable (the Matlab script 'mkplotComp_V1.m' shows how these distances are converted to depths along the DTS pole). The NetCDF file for the EC electrode data contains the measured temperature and EC values (converted to 25 ^oC), as well as the converted salinity data, against the time and the sensor positions within the solar pond. The NetCDF file for the density data contains the measured density data at two times during the modeling period for the sampling locations within the solar pond. In all cases, the dates and times are reported as Matlab time numbers (days since the start of the year 0 AD). The axis definition for the distances x, y, and z within the solar pond is as reported in Figure 1.

4 Results

This data set presents the results as movies. This document briefly presents the results obtained from the model simulations in the Figures 2 until 4. For an extensive discussion, we refer to the accompanying article.

Figure 2 shows the provided output parameters of the model after 72 hours. Plots like these can be created with the Matlab routine that is available in this data set. The water level excitations due to density gradient flows (Figure 2a), which in the free surface simulations reach a maximum of 2 mm, are an important feature of the non-hydrostatic model. The velocity profiles show the onset of convection cells along the sloping wall (Figure 2b). One can also see the salinity and temperature profiles change over time (Figures 2c and d).

Figure 3 compares the modeled temperatures and salinities of the free surface and rigid-lid simulations with the point data obtained by the EC probes and the vertical temperature profile obtained by the DTS pole. The movie in this data set shows the complete temporal evolution of these vertical profiles for:

- the complete free surface simulations;

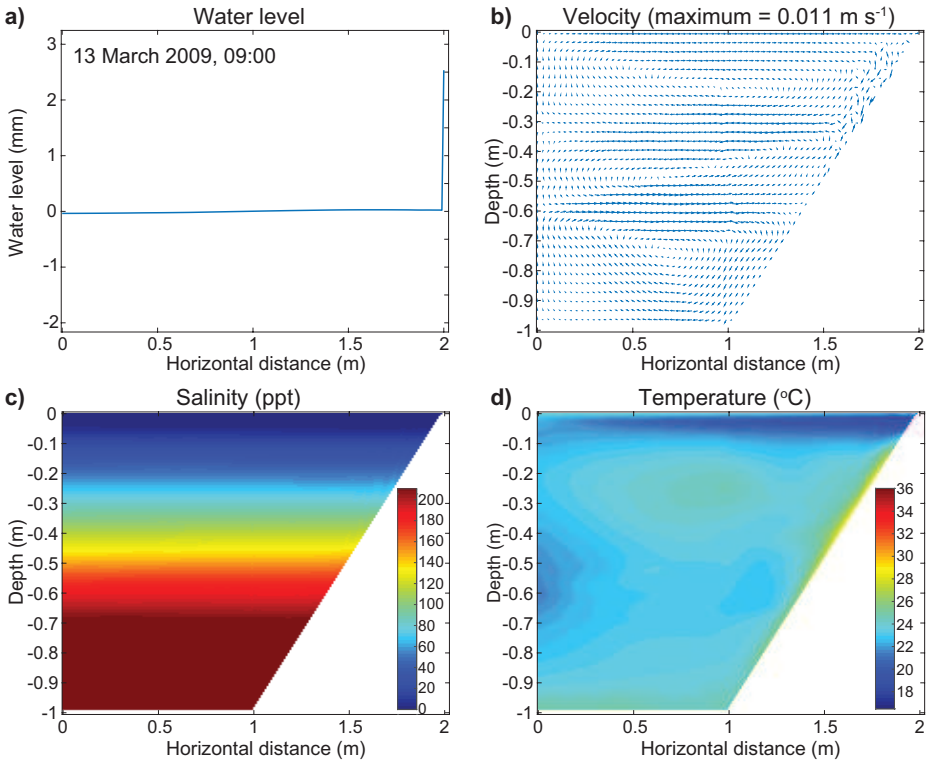

Figure 2: General overview of the output parameters of the model after 72 hours (13 March 2009, 9:00 LT), with a) the water level (m), b) the velocity vectors combining the horizontal and vertical flow velocities ($m\,s^{-1}$), c) the salinity (weight-‰), and d) the temperature (^oC).

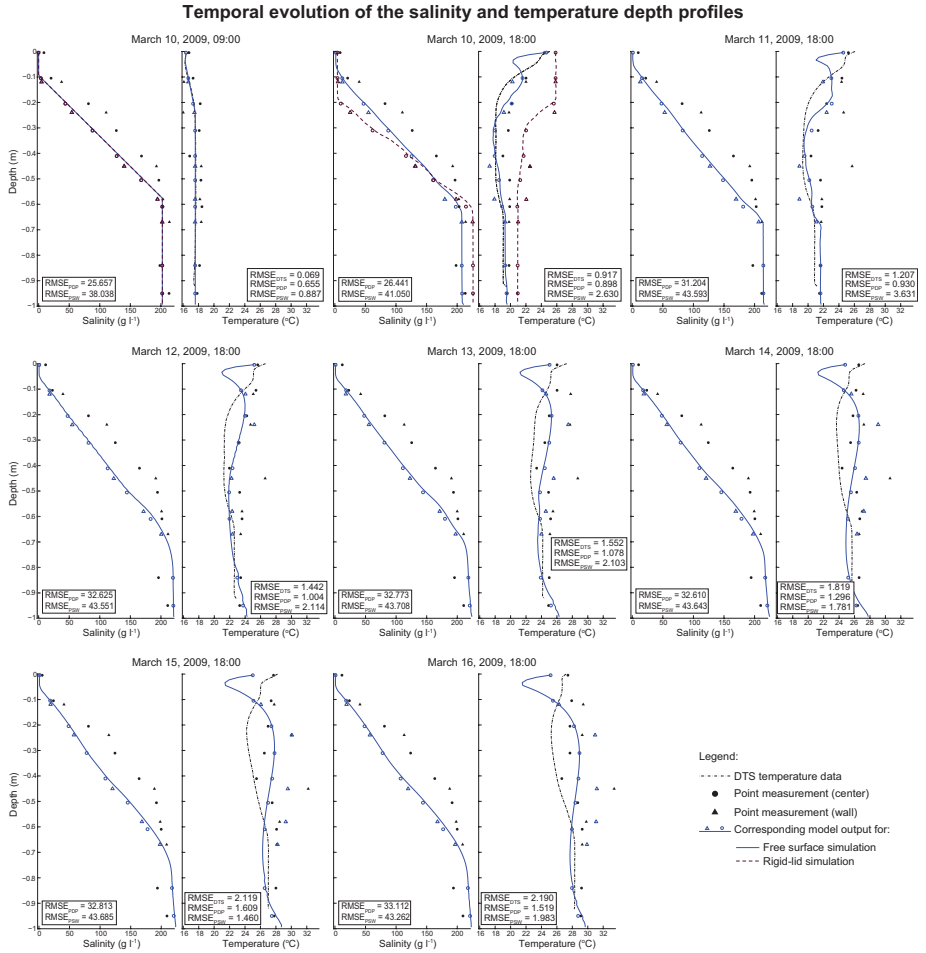

Figure 3: A comparison between the evolution of the modeled and measured salinity and temperature profiles over the simulation period. The measurement data are presented for point measurements at different depths above the flat bottom (filled circles) and at different depths along the sloping wall (filled triangles), as well as a vertical DTS temperature profile above the flat bottom (the black dash-dot line). The corresponding model output data is presented as a blue solid line and blue open circles and triangles for the free surface simulations, and as a purple dashed line and purple open circles and triangles for the rigid-lid simulations.

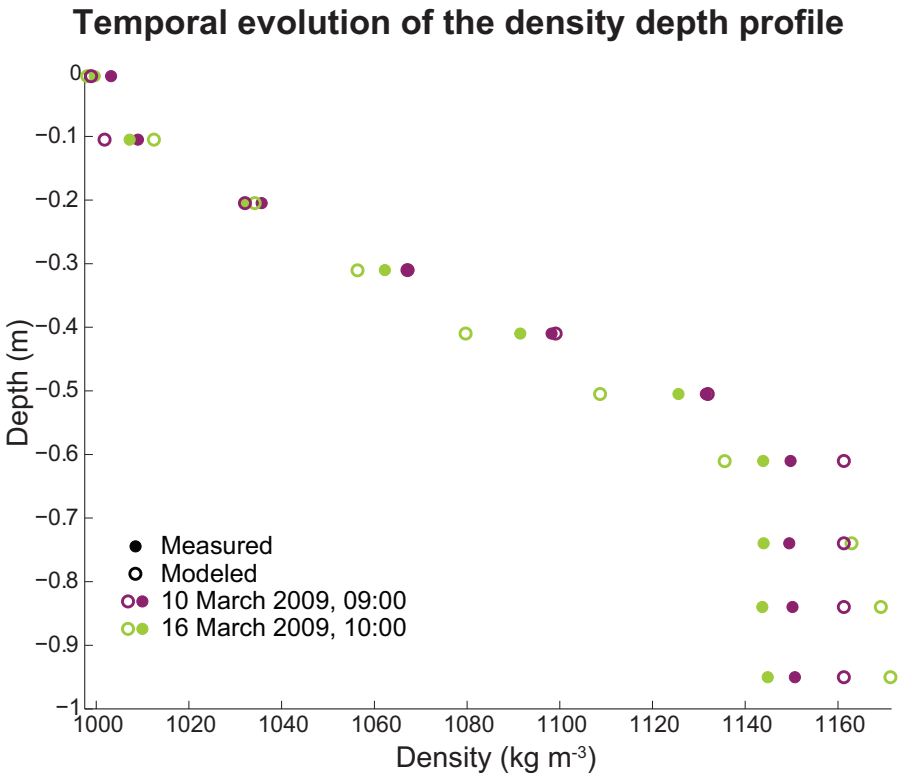

Figure 4: A comparison between the modeled (open circles) and measured (filled circles) density profiles at the start of the simulation period (purple) and after six days (green).

- the comparison between the free surface simulations and the rigid-lid simulations for the duration of the rigid-lid simulations.

Figure 4 shows the comparison of the modeled and measured densities at the locations where the water density samples were taken. The modeled densities are calculated from the modeled temperatures and salinities with the updated Eckart formula by Wright (1997).

References

Adams, E. E., Cosler, D. J., Helfrich, K. R., 1990. Evaporation from heated water bodies: Predicting combined forced plus free convection. Water Resources Research 26 (3), 425–435.
URL `http://dx.doi.org/10.1029/WR026i003p00425`

Eckart, C. H., 1958. The equation of state of water and sea water at low tem-

peratures and pressures, part 2 of properties of water. American Journal of Science 256 (4), 225–240.

Henderson-Sellers, B., 1986. Calculating the surface energy balance for lake and reservoir modeling: A review. Reviews of Geophysics 24 (3), 625–649.
URL http://dx.doi.org/10.1029/RG024i003p00625

Kim, K. S., Chapra, S. C., 1997. Temperature model for highly transient shallow streams. Journal of Hydraulic Engineering 123 (1), 30–40.
URL http://dx.doi.org/10.1061/(ASCE)0733-9429(1997)123:1(30)

Rabl, A., Nielsen, C. E., 1975. Solar ponds for space heating. Solar Energy 17 (1), 1 – 12.
URL http://www.sciencedirect.com/science/article/pii/0038092X75900110

Stelling, G. S., Zijlema, M., 2010. Numerical Modeling of Wave Propagation, Breaking and Run-Up on a Beach. Springer Berlin Heidelberg, Berlin, Heidelberg, pp. 373–401.
URL http://dx.doi.org/10.1007/978-3-642-03344-5_13

Suárez, F., Childress, A., Tyler, S., 2010. Temperature evolution of an experimental salt-gradient solar pond. Journal of Water and Climate Change 1 (4), 246–250.

SWASH source code (Version 1.20), 2011. http://swash.sourceforge.net/, accessed on: 30 may 2016.
URL http://swash.sourceforge.net/

Thomann, R. V., Mueller, J. A., 1987. Principles of surface water quality modeling and control. Harper & Row, Publishers.

Unesco, 1981. Tenth report of the joint panel on oceanographic tables and standards. UNESCO Tech. Paper in Marine Science 36, 25.

Washburn, E. W., West, C. J., 1933. International Critical Tables of Numerical Data, Physics, Chemistry and Technology: Vol. 1-7. McGraw-Hill.

Wright, D. G., Jun. 1997. An equation of state for use in ocean models: Eckart's formula revisited. J. Atmos. Oceanic Technol. 14 (3), 735–740.
URL http://dx.doi.org/10.1175/1520-0426(1997)014<0735:AEOSFU>2.0.CO;2

Zijlema, M., Stelling, G., Smit, P., 2011. Swash: An operational public domain code for simulating wave fields and rapidly varied flows in coastal waters. Coastal Engineering 58 (10), 992 – 1012.
URL http://www.sciencedirect.com/science/article/pii/S0378383911000974